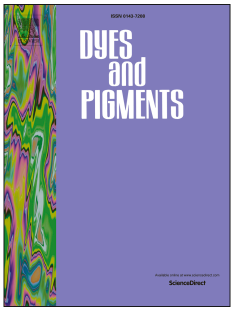

Synthesis of cyanovinyl thiophene with different acceptor containing organic dyes towards high efficient dye sensitized solar cells

Subbaiah Manoharan, Jerry J. Wu, Sambandam Anandan

PII: S0143-7208(16)30251-0
DOI: 10.1016/j.dyepig.2016.05.052
Reference: DYPI 5284

To appear in: *Dyes and Pigments*

Received Date: 21 March 2016
Revised Date: 5 May 2016
Accepted Date: 31 May 2016

Please cite this article as: Manoharan S, Wu JJ, Anandan S, Synthesis of cyanovinyl thiophene with different acceptor containing organic dyes towards high efficient dye sensitized solar cells, *Dyes and Pigments* (2016), doi: 10.1016/j.dyepig.2016.05.052.

Graphical Abstract

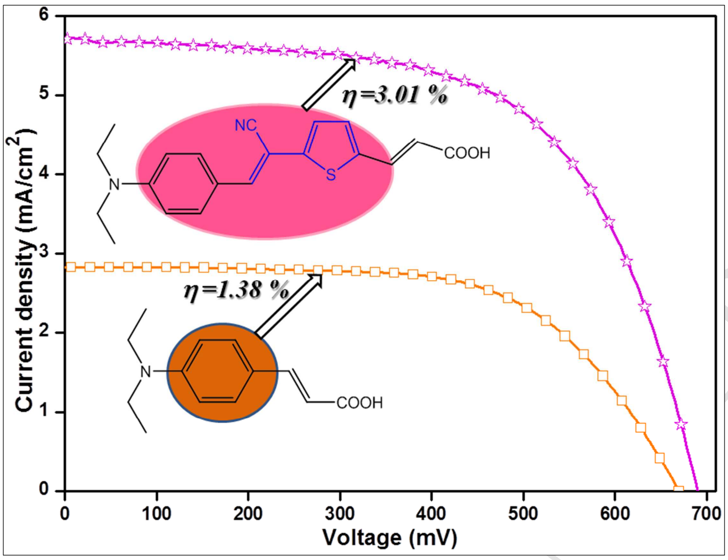

Synthesis of Cyanovinyl Thiophene with Different Acceptor Containing Organic Dyes towards High Efficient Dye Sensitized Solar Cells

Subbaiah Manoharan[a], **Jerry J. Wu**[b,*], **Sambandam Anandan** [a,,b,*,*]

[a]*Nanomaterials and Solar Energy Conversion Laboratory, Department of Chemistry,*
National Institute of Technology, Trichy-620 015, India

[b]*Department of Environmental Engineering and Science, Feng Chia University, Taichung*
407, Taiwan

* To whom the correspondence should be addressed: E-mail: sanand@nitt.edu;
sanand99@yahoo.com; Tel.: 91-431-2503639; Fax: 91-431-2500133

Abstract

A series of donor-π-acceptor (D-π-A) metal-free organic dyes employing a diethylamine moiety as donor, phenyl with and without cyanovinyl thiophene unit as a π-spacer and acrylic acid, rhodanine-3-acetic acid, and benzimidazole-5-carboxylic acid as acceptor/anchor, have been designed and synthesized through simple synthetic procedures and investigated as photosensitizers for the dye-sensitized solar cell (DSSC) application. The effects of both the π-spacer and an acceptor modification upon the optoelectronic properties, theoretical and photovoltaic properties of the dyes were studied. In general, DSSCs fabricated with the dyes containing cyanovinyl thiophene unit as a π-spacer shows more than two times higher efficiency than the DSSCs fabricated without cyanovinyl thiophene unit. The maximum power conversion efficiency of 3.01 % was achieved for the cyanovinyl thiophene unit in the π-spacer and acrylic acid acceptor dye based DSSC.

Keywords: cyanovinyl thiophene, π-spacer, Dye-sensitized solar cell, acceptor, organic dye, optoelectronic properties

1. Introduction

From the beginning of the last century, our energy demand has grown tremendously as a result of the rapid population growth along with their higher living standards. The most viable way for producing clean energy is through solar cell technology due to its sustainability and abundant supply of solar energy. After seminal report by O'Regan and Gratzel in 1991[1], Dye-sensitized solar cells (DSSCs) have attracted lots of attention for their use in next-generation solar cell technologies owing to their multiple advantages, such as mechanical flexibility, light weight, high efficiency, and cost-effective fabrication method [2; 3]. As a critical component in DSSCs for improving the efficiency, the metal-free organic chromophores have a great deal of interest in the last decades for many researchers due to their simple synthesis procedures and easy purification, high molar extinction coefficients, environmental concerns, and tunable structural modification. The extensively studied metal free organic dyes usually contain donor (D) and acceptor (A) groups bridged by the π-conjugated unit (D–π–A). This is because of their intramolecular charge transfer processes and easy to design new dye structures for adjusting the energy levels and extend the absorption spectra [4; 5]. In the past decades, a large variety of aromatic compounds containing nitrogen atom were studied as a donors, such as coumarin, triarylamine, indoline, carbazole, N,N-dialkylaniline, phenothiazine, etc. Compared to the donors, π-conjugated units and acceptors were studied very limited in the metal free organic dyes. The π-conjugated unit not only extends the absorption wavelength in the visible region, but also affects the rate of internal charge recombination and the electron injection from excited dyes to the semiconductor surface [6; 7]. Hence, the π-conjugated unit modification plays a crucial role in the designing of metal free organic dyes for obtaining better DSSC performance. Widely used π-conjugated units are thiophene derivatives because of their intrinsic charge transport behavior, environmental and chemical stability as well as structural versatility [8;

9]. However, the introduction of thiophene derivative is very complicated because their synthetic procedure consumes very expensive metal catalysts and the reaction conditions are very rigorously anhydrous and inert [10; 11]. To avoid such problems, thiophene-2-acetonitrile was chosen as a starting material and by Knoevenagel Condensation reaction, where the thiophene derivative is easily introduced. Further in such processes, it does not need of expensive catalysts and also it follows simple reaction conditions. This synthetic route has another merit, i.e. the cyanovinyl group introduced along with thiophene moiety leads to extended π-conjugation and also reduces the gap between HOMO and LUMO energy levels. In addition, the need of the acceptor modification in this cyanovinyl thiophene based dyes were carried out for getting high solar cell performance. In this regard, acrylic acid, rhodanine-3-acetic acid, and benzimidazole-5-carboxylic acid were chosen.

On the basis of the foregoing points, a series of six metal free organic dyes, based on N,N-diethylamine as a donor, phenyl with and without cyanovinyl thiophene as a π-conjugation unit and acrylic acid, rhodanine-3-acetic acid, and benzimidazole-5-carboxylic acid as an acceptor were synthesized (as shown in scheme 1) which are namely 3-(4-(diethylamino)phenyl)acrylic acid (EC), 3-(5-(1-cyano-2-(4-(diethylamino)phenyl)vinyl) thiophen-2-yl)acrylic acid (ETC), 2-(5-(4-(diethylamino)benzylidene)-4-oxo-2-thioxothiazolidin-3-yl)acetic acid (ER), 2-(5-((5-(1-cyano-2-(4-(diethylamino) phenyl)vinyl)thiophen-2-yl)methylene)-4-oxo-2-thioxothiazolidin-3-yl)acetic acid (ETR), 2-(4-(diethylamino)phenyl)-benzimidazole-5-carboxylic acid (EB), and 2-(5-(1-cyano-2-(4-(diethylamino)phenyl)vinyl)thiophen-2-yl)-1H-benzimidazole-5-carboxylic acid (ETB). Therefore in this article, the effects of π-conjugated unit and acceptor towards metal free organic dyes on the photophysical, electrochemical, theoretical properties, and DSSC performance of the dyes have been investigated orderly. This result strongly implies that along with π-conjugated unit acceptor modification also plays an important role for constructing the high efficient organic dyes for DSSCs.

2. Experimental Section

2.1. Materials and Methods

Thiophene-2-acetonitrile (Sigma-Aldrich), 4-diethylaminobenzaldehyde (Alfa Aesar), 3,4-diaminobenzoic acid (Alfa Aesar), Rhodanine-3-aceticacid (Sigma-Aldrich), Malonic acid (Alfa Aesar), Copper (II) acetate ($Cu(OAc)_2$) (Sigma-Aldrich), and Tetrabutylammonium perchlorate (TBAP) (Sigma-Aldrich) were purchased and used without further purification. Phosphorus oxychloride ($POCl_3$), *N*,*N*-dimethylforamide (DMF), Ammonium acetate, glacial acetic acid, piperidine and nitrobenzene were purchased from Merck. ^{1}H and ^{13}C NMR analysis were measured on Bruker 500 MHz NMR Spectrometer in deuterated chloroform or dimethylsulfoxide solution at 298K. Chemical shifts (δ values) were recorded in units of ppm relative to tetramethylsilane (TMS) as an internal standard. High-resolution mass spectra were obtained by ESI using Orbitrap mass spectrometer. The FT-IR spectra were obtained with a Thermo Scientific Nicolet iS5 FT-IR spectrometer. All reactions were monitored by using TLC plates. All chromatographic separations were carried out on silica gel (60–130 mesh).

2.2. Photophysical and electrochemical measurements

Absorption and fluorescence spectra were measured in DMF solution on a T90+ UV-vis spectrometer and Shimadzu RF-5301 PC spectrofluorophotometer, respectively. Electrochemical measurements were performed on a Metrohm Autolab PGSTAT potentiostat/galvanostat-84610. All measurements were carried out at room temperature with a conventional three-electrode configuration consisting of a glassy carbon (GC) working electrode, a platinum wire auxiliary electrode, and a silver wire used as the quasi-reference electrode. The potentials were reported vs. ferrocene as standard using a scan rate of 0.1 Vs^{-1}. The CV experiments were performed with 3×10^{-4} M dye solution and 0.1 M tetrabutylammonium perchlorate (TBAP) in anhydrous DMF as a supporting electrolyte under Argon atmosphere. Electrochemical impedance spectroscopy (EIS) measurements were done under 85 mW/cm^2 light illumination with a frequency ranging between 10 kHz to 0.1 Hz at their open circuit potential (OCP) by using an Autolab PGSTAT potentiostat/galvanostat-84610.

2.3. Synthesis

2.3.1. 3-(4-(diethylamino)phenyl)-2-(thiophen-2-yl)acrylonitrile (1a)

4-diethylaminobenzaldehyde (2 g, 11.3 mmol) and thiophene-2-acetonitrile (1.44 mL, 13.6 mmol) were taken in a two neck round bottom flask containing 30 mL freshly distilled ethanol. 6 M NaOH (0.1 mL) was added to this reaction mixture at room temperature after that the resulting mixture was refluxed for 2 h. After cooling to room temperature, the mixture was poured into water and extracted with chloroform. The collected organic extracts were dried by Na_2SO_4. The solvent was removed under vacuum and the residue was further purified by column chromatography on silica gel by using a hexane as an eluent to give orange yellow color solid with yield 78.40% (2.5 g). ^{1}H NMR ($CDCl_3$, ppm): δ 1.24 (t, 6H), 3.43-3.47 (q, 4H), 6.69-7.82 (ArH, 7H). ^{13}C NMR ($CDCl_3$, ppm): δ 12.62, 44.53, 111.18, 118.43, 120.45, 124.29, 127.89, 131.45, 140.50, 140.76, 149.37. IR (KBr pellet, cm^{-1}): 3096, 2970, 2897, 2207, 1605, 1575, 1406, 1341, 1272, 1196, 1153, 1076, 1015, 848, 808, 712. Anal. Calcd. for $C_{17}H_{18}N_2S$: C, 72.30; H, 6.42; N, 9.92. Found: C, 72.18; H, 6.62; N, 9.87. HRMS (ESI): Anal. Calcd. for $C_{17}H_{18}N_2S$: 282.1263. Found: 283.1259 $[M+H]^+$.

2.3.2. 3-(4-(diethylamino)phenyl)-2-(5-formylthiophen-2-yl)acrylonitrile (1b)

Freshly distilled DMF (4.4 mL, 57 mmol) and $POCl_3$ (5.4 mL, 57 mmol) were taken in a 3-neck round bottom flask under N_2 atmosphere at 0 °C, and then it was stirred for 1 h. 2 g (7.1 mmol) of compound 1a dissolved in 1,2-dichloroethane (20 mL) was added drop-wise to the above solution and the resulting mixture was stirred for 3 h at 95 °C. After cooled to room temperature, the mixture was poured into crushed ice and basified with 6 M NaOH. It was then extracted by dichloromethane and the organic layer was dried under Na_2SO_4. After evaporating the organic solvent, the crude product was purified by column chromatography on silica gel using a mixture of Ethyl acetate/Hexane (v/v = 2/100), to give a maroon color solid with yield 22.74% (0.5 g). ^{1}H NMR ($CDCl_3$, ppm): δ 1.24 (t, 6H, J=6.5 Hz, 7 Hz), 3.43-3.48 (q, 4H, J=7 Hz), 6.71 (d, 2H, J=6.5 Hz), 7.32 (d, 1H, J=3.5 Hz), 7.39 (s, 1H), 7.69 (d, 1H, J=3.5 Hz), 7.85 (d, 2H, J=8 Hz), 9.84 (s, 1H). ^{13}C NMR ($CDCl_3$, ppm): δ 12.57, 44.79, 96.91, 111.43, 117.71, 125.17, 132.54, 137.35, 141.25, 143.54, 150.24, 150.72, 182.30. IR (KBr pellet, cm^{-1}): 3086, 2964, 2870, 2210, 1653, 1601, 1562, 1514, 1440, 1410, 1356, 1276, 1221, 1190, 1157, 1053, 1005, 942, 897, 810, 704. Anal. Calcd. for $C_{18}H_{18}N_2OS$: C, 69.65; H, 5.84; N, 9.02. Found: C, 69.50; H, 5.92; N, 9.00. HRMS (ESI): Anal. Calcd. for $C_{18}H_{18}N_2OS$: 310.1208. Found: 311.1213 $[M+H]^+$.

2.3.3. 3-(5-(1-cyano-2-(4-(diethylamino)phenyl)vinyl)thiophen-2-yl)acrylic acid (ETC)

A 25 mL two-neck round bottom flask was charged with 0.15 g (0.48 mmol) of compound 1b, 0.15 g (1.45 mmol) of malonic acid, and 3 mL pyridine. Then the reaction mixture was refluxed for 5 h in the presence of piperidine (0.052 mL, 0.53 mmol). After cooling to room temperature, the mixture was poured into ice water followed by acidified with dilute HCl solution. The precipitate was filtered, washed with distilled water, and then kept drying under vacuum for 10 h. After drying under vacuum, the precipitate was purified by recrystallization from ethanol to afford pure red solid in 76.43 % yield (0.13 g). ^{1}H NMR (DMSO-d_6, ppm): δ 1.13 (t, 6H, J=6.5 Hz, 6 Hz), 3.43-3.47 (q, 4H, J=7 Hz), 6.13 (d, 1H, J=15.5 Hz), 6.78 (s, 2H), 7.25 (s, 1H), 7.35 (d, 1H, J=3.5 Hz), 7.48 (s, 1H), 7.59 (d, 1H, J=3.5 Hz), 7.71 (d, 1H, J=16 Hz), 7.83 (s, 2H). ^{13}C NMR (DMSO-d$_6$, ppm): δ 12.91, 44.37, 111.73, 117.93, 118.61, 119.95, 123.82, 125.36, 133.15, 134.88, 136.78, 138.03, 142.52, 146.53, 150.19, 168.02. IR (KBr pellet, cm^{-1}): 3424, 3086, 2978, 2928, 2208, 1679, 1608, 1565, 1517, 1408, 1356, 1277, 1195, 1155, 1080, 1014, 969, 807. Anal. Calcd. for $C_{20}H_{20}N_2O_2S$: C, 68.16; H, 5.72; N, 7.95. Found: C, 68.20; H, 5.75; N, 7.90. HRMS (ESI): Anal. Calcd. for $C_{20}H_{20}N_2O_2S$: 352.1318. Found: 353.1317 [M+H]$^+$.

2.3.4. 2-(5-((5-(1-cyano-2-(4-(diethylamino)phenyl)vinyl)thiophen-2-yl)methylene)-4-oxo-2-thioxothiazolidin-3-yl)acetic acid (ETR)

0.15 g (0.48 mmol) of compound 1b and 0.097 g (0.50 mmol) of rhodanine-3-acetic acid were added to 25 mL two-neck round bottom flask containing 20 mL of acetic acid. The reaction mixture was refluxed for 3 h in the presence of ammonium acetate 0.088 g (1.14 mmol). After cooling to room temperature, the mixture was poured into ice water. The precipitate was filtered and washed with distilled water. After drying under vacuum, the precipitate was recrystallized from ethanol to yield red colour solid (yield: 0.142 g, 60.83 %). ^{1}H NMR (DMSO-d_6, ppm): δ 1.15 (t, 6H, J=7 Hz), 3.44-3.49 (q, 4H, J=7 Hz), 4.73 (s, 2H), 6.68 (d, 1H, J=9 Hz), 7.42 (t, 1H, J=3.5 Hz), 7.74 (s, 1H), 7.78 (d, 1H, J=3.5 Hz), 7.90 (d, 2H, J=9.5 Hz), 8.13 (s, 1H). ^{13}C NMR (DMSO-d_6, ppm): δ 12.85, 44.33, 45.62, 111.18, 118.51, 119.92, 123.71, 125.39, 128.73, 130.25, 131.71, 132.16, 135.69, 142.24, 143.43, 149.85, 150.06, 168.26. IR (KBr pellet, cm^{-1}): 3388, 3095, 2972, 2928, 2208, 1708, 1606, 1567, 1517, 1433, 1406, 1351, 1240, 1190, 1156, 1108, 1066, 1049, 948, 891, 819, 795, 746, 622. Anal. Calcd. for $C_{23}H_{21}N_3O_3S_3$: C, 57.12; H, 4.38; N, 8.69. Found: C, 57.13; H, 4.40; N, 8.65. HRMS (ESI): Anal. Calcd. for $C_{23}H_{21}N_3O_3S_3$: 483.0818. Found: 484.0819 [M+H]$^+$.

2.3.5. 2-(5-(1-cyano-2-(4-(diethylamino)phenyl)vinyl)thiophen-2-yl)benzimidazole-5-carboxylic acid (ETB)

A mixture of 3,4-diaminobenzoic acid (0.12 g, 0.81 mmol) and compound 1b (0.25 g, 0.81 mmol) were added to 25 mL two-neck round bottom flask containing 3.5 mL nitrobenzene. The reaction mixture was heated at 155-160 °C for 20 h. After cooled to room temperature, the crude product was diluted with diethyl ether (Et_2O). The solids were filtered, washed with Et_2O and vacuum dried to get 0.28 g of red colour solid with 78.87% yield. ^1H NMR (DMSO-d_6, ppm): δ 1.08 (t, 6H), 3.37 (q, 4H), 6.53-8.21 (ArH, 10H), 13.38 (s, 1H). ^{13}C NMR (DMSO-d_6, ppm): δ 12.85, 44.33, 111.18, 118.51, 119.92, 123.71, 125.39, 128.73, 130.25, 131.71, 132.93, 135.69, 142.24, 143.43, 149.85, 150.66, 168.26. IR (KBr pellet, cm^{-1}): 3443, 3082, 2979, 2934, 2208, 1671, 1608, 1560, 1517, 1409, 1355, 1272, 1192, 1155, 1077, 1013, 964, 891, 810, 715. Anal. Calcd. for $C_{25}H_{22}N_4O_2S$: C, 67.85; H, 5.01; N, 12.66. Found: C, 67.90; H, 5.05; N, 12.60. HRMS (ESI): Anal. Calcd. for $C_{25}H_{22}N_4O_2S$: 442.1536. Found: 443.1536 $[M+H]^+$.

2.3.6. Synthesis of relevant dyes without cyanovinyl thiophene (EC, ER and EB)

3-(4-(diethylamino)phenyl)acrylicacid (EC), 2-(5-(4-(diethylamino)benzylidene)-4-oxo-2-thioxothiazolidin-3-yl) acetic acid (ER) and 2-(4-(diethylamino)phenyl)benzimidazole-5-carboxylic acid (EB) dyes were synthesized from 4-(diethylamino)benzaldehyde according to the reported procedures available in the literature [12; 13].

2.4. Device fabrication and Photovoltaic measurements

A fluorine-doped SnO_2 conducting glass (FTO; sheet resistance 10 Ω $sq.cm^{-1}$; brought from BHEL, INDIA) was cleaned with double distilled water and acetone. The TiO_2 paste was coated on the cleaned conducting glass substrate according to the described procedure [14]. The active area was 1 x 1 cm^2. After heating the TiO_2 thin film up to 80° C, the film was soaked in a DMF solution containing 0.3 mM sensitizers for 24 h at room temperature for the dye adsorbed on the TiO_2 surfaces. A platinized FTO was prepared by chemical deposition of 0.05 M hexachloroplatinic acid in isopropanol which acts as a counter electrode

[15]. After being rinsed with DMF, the photoanode was placed on top of the counter electrode and tightly clipped it to form a cell. The electrolyte was composed of 0.5 M LiI, 0.05 M iodine (I_2) and 0.5 M 4-tert-butylpyridine (TBP) in 3-methoxypropionitrile which was injected in between the two electrodes.

The photoelectrochemical characterizations was measured by using modified light source 300 W Xe lamp (Oriel, 6258) equipped with a AM 1.5 filter (Oriel, 81080 kit) and the light intensity was 85 mW/cm^2. The photocurrent-voltage characteristics of the DSSCs were recorded with an Autolab potentiostat/galvanostat-84610. The spectra of monochromatic incident photon-to-current conversion efficiency (IPCE) as a function of wavelength were measured for the solar cells with an Enlitech QE-T spectral response measurement system. An RC-S103011-E standard single crystal Si solar reference cell was used to calibrate the IPCE measurement spectrum.

3. Results and discussion

3.1. Synthesis and Characterization

Molecular structures and synthetic protocol used to obtain the desired organic dyes (EC, ER, EB, ETC, ETR and ETB) were shown in the Scheme 1. 3-(4-(diethylamino)phenyl)-2-(thiophen-2-yl)acrylonitrile (1a) and 3-(4-(diethylamino)phenyl)-2-(5-formylthiophen-2-yl)acrylonitrile (1b) were synthesized by well-known reactions, such as Knoevenagel and Vilsmeier-Haack formylation reaction. Later compound (1b) was successfully converted to the desired dyes (ETC and ETR) on treatment with active methylene compounds, such as malonic acid and rhodanine-3-acetic acid by Knoevenagel Condensation reaction. The dye ETB was synthesized by performing condensation reaction of compound (1b) with 3,4-diaminobenzoic acid in the presence of nitrobenzene. Like-wise, relevant dyes without cyanovinyl thiophene moiety (EC, ER and EB) were synthesized for comparison purpose. Synthesized dyes were thoroughly characterized by FT-IR, ^{1}H and ^{13}C

NMR, and mass spectral methods. In the ^{1}H NMR spectra of compound (1a), the aldehyde hydrogen peak (chemical shift value around 9-10 ppm) was disappeared and new peaks appear at 7.82 and 7.81 ppm, which corresponds to the newly formed benzylic hydrogen and hydrogen present in the thiophene unit. In the compound (1b) the new peak at 9.84 ppm corresponds to the aldehyde hydrogen at thiophene unit. Thus, the NMR analysis conform the compound 1a and 1b product formation. In the ^{1}H NMR spectra of ETC and EC dyes, the aldehyde hydrogen peak (chemical shift value around 9-10 ppm) was disappeared and new peaks appeared at 6.2 and 7.7 ppm with coupling constant of 16 Hz which implies that the newly formed double bond (C=C) exist in *E*-conformation. Similarly, in the ^{1}H NMR spectra of ETR and ER, a peak appear at 7.4 ppm region which corresponds to the hydrogen present in the newly formed C=C double bond. Likewise in the ^{1}H NMR spectra of ETB and EB dye, a new peak was seen at chemical shift value around 13 ppm, corresponding to the –NH hydrogen in the benzimidazole moiety. The ^{13}C NMR results were also an effective support for the ^{1}H NMR results. Thus, the NMR analysis conform the desired end product formation. In addition, the observed FT-IR and mass spectra of synthesized dyes also supports such product formation.

3.2. Photophysical properties

To find out the π–spacer and acceptor effect on the optical properties of the synthesized dyes, the electronic absorption and fluorescence emission spectral studies were performed in DMF medium ($5x10^{-5}$ M). The optical parameters deduced from these spectral studies were listed in Table 1 and their corresponding spectra were displayed in Figure 1. All the synthesized dyes exhibit two distinct absorption bands: one weak band in the ultraviolet region (280 to 340 nm) corresponding to the π-π* electronic transitions and the strong absorption band lying in the visible region (350 to 531 nm) that can be assigned to an intramolecular charge transfer (ICT) between the donor unit and the acceptor end group. The absorption spectra are red-shifted (~60 nm) and expanded when the cyanovinyl thiophene π–spacer is introduced to the dye molecules (ETC, ETR and ETB), compared to the relevant dyes without such π–spacer unit (EC, ER and EB) which clearly indicates that the insertion of cyanovinyl thiophene unit in between the donor and acceptor, increases the π-bridge length and also the electron withdrawing nature of acceptor [16; 17]. Similarly, the molar extinction coefficient of the cyanovinyl thiophene containing dyes shows ~10,000 $M^{-1}cm^{-1}$ higher than that of the dyes without such group, which is also due to the lengthening of π-conjugation and increasing the electron withdrawing ability of acceptor. This property may be responsible towards enhancing the light harvesting ability and photocurrent generation in DSSC [18; 19].

Among the synthesised dyes, rhodanine-3-acetic acid acceptor based dyes (ER and ETR) show high maximum absorption wavelength (λ_{max}) with highest molar extension coefficient (ε) compared to the corresponding dyes with carboxylic acid (EC and ETC) and benzimidazole-5-carboxylic acid (EB and ETB) acceptor. This may be due to extension of π–conjugated system with strong electron withdrawing ability were found when rhodanine-3-acetic acid as acceptor [20; 21]. In the photoluminescence spectra, all the synthesized dyes were excited at their absorption maximum. All the dyes exhibited strong luminescence maxima in the wavelength range of 445–662 nm, respectively. The emission spectra also follow the same trend like absorbance spectra. Stokes shift calculation of these two set of dyes revealed that cyanovinyl thiophene unit containing dyes shows greater shift (in the range of 80-131 nm) than dyes without such group (in the range of 69-80 nm), which indicates that the insertion of cyanovinyl thiophene unit enhances the charge transfer nature of the excited state [22; 23]. The insertion of cyanovinyl thiophene unit reduces the planar structure of the dye molecule which may be the reason for the observed larger Stokes shifts [24]. The optical band gap (E_{0-0}) of synthesized dyes were derived from the intersection of normalized absorption and emission spectra [25] and illustrated in Table 1. Due to the change in the conjugation length and electron withdrawing nature of the acceptor, the band gap of the synthesized dyes get decreased which may be responsible for broadening of absorption peak and in addition harvesting higher light efficiency [26; 27].

3.3. Electrochemical measurements

To find out the electrochemical behaviour of the synthesized dyes, the cyclic voltammetry (CV) was carried out in a solution of 0.1 M TBAP in DMF medium in order to illustrate the thermodynamic feasibility of electron injection from the excited dye molecule to the TiO_2 conduction band and dye regeneration through electrolyte. The summarized CV data are presented in Table 1 and the representative cyclic voltammograms are shown in Figure 2. The HOMO energy level can be calculated from the onset oxidation potential [E_{ox} (onset)] based on the reference energy level of ferrocene (4.8 eV below the vacuum level) and using the relationship of HOMO = − [E_{ox} (onset) − E_{FC} + 4.8] eV, where in E_{FC} is the potential of the internal standard, the ferrocene/ferricenium ion (Fc/Fc^+) couple [28]. The value of E_{FC}, determined under such experimental conditions, was about 0.53 V vs Ag electrode. The LUMO energy was obtained by the addition of zero-zero energy (E_{0-0}) and HOMO.

All the dyes show one irreversible peak arising from the oxidation potential around 0.60 to 1 V, which is due to the removal of electron from the donor amine moiety. Noticed negative shift in the oxidation potential for cyanovinyl thiophene unit containing dyes (ETC, ETR and ETB) upon compared to the corresponding dyes without such unit (EC, ER and EB) could be attributed to the expansion of their π-conjugated units by linking a cyanovinyl thiophene unit [29].

The schematic energy levels (HOMO and LUMO) of synthesized dyes, conduction band of TiO_2, and redox potential of I^-/I_3^- are illustrated in Figure 3. Inserting the cyanovinyl thiophene unit as the π-spacer between the donor moiety and anchoring group may be beneficial in bringing down the LUMO energy level closer to TiO_2 conduction band and lift up the HOMO energy level closer to the electrolyte potential thus leads to band gap narrowing in the synthesized dyes. The calculated LUMO values of all dyes were found in the range -1.93 to -3.00 eV, which is above than the conduction band edge of TiO_2 (-4.0 eV vs vacuum) [30]. This should be sufficient for down-hill electron injection process from the excited dye molecule into the conduction band of TiO_2. The HOMO values of dyes were also found in between -4.90 to -5.23 eV (lower than the I^-/I_3^- redox couple; -4.6 eV vs vacuum) [31] which ensures favourable dye regeneration through combination between the oxidized dye and I^- ions in the electrolyte.

3.4. Molecular orbital calculations

To obtain a further insights and better understanding of the molecular geometrical structures and electron distributions in the frontier orbitals of synthesized dyes, the density functional calculations were carried out by using the B3LYP exchange-correlation functional and the d-polarized 6-31G (d) basis set implemented in Gaussian 09 program [32-34]. Figure 4 shows the optimized structure and the frontier orbitals (HOMO and LUMO) of the dyes.

The optimized dye structures reveals that the introduction of cyanovinyl thiophene unit in the synthesized dyes (ETC, ETR, and ETB) bent the geometry of the molecules, which reduce the aggregation of dye molecules on TiO_2 surface [35; 36]. The HOMO levels of acrylic acid (EC and ETC) and benzimidazole-5-carboxylic acid (EB and ETB) acceptor based dyes are homogeneously distributed on the electron donating amine moieties and the π–spacer, whereas LUMO levels are delocalized through the π–spacer and acceptor. Such spatial separation in HOMO and LUMO orbitals through π-bridge is an important characteristic for D-π-A organic dyes in DSSCs. Such result indicates that upon illumination of light the electron density may effectively move from the donor moiety to the acceptor segment in the HOMO-LUMO excitation, which leads to the fast electron injection from LUMO to the conduction band of TiO_2 [37].

However in the case of rhodanine-3-acetic acid as acceptor dye (ER and ETR), the HOMO and LUMO levels were majorly populated especially on the sulfur and thiocarbonyl group, and due to the presence of -CH_2- group (broken conjugation), the anchoring -COOH group in LUMO level gets isolated which may render anchoring group, and the π–spacer in two different planes [38]. Consequently, it prevents electrons injected into the TiO_2 conduction band via the carboxyl group, which lowers short circuit current density and in turn solar cell efficiency.

3.5. Photovoltaic Performance

The typical investigation of photovoltaic characteristics of fabricated DSSCs were sensitized with synthesized dyes on nanocrystalline TiO_2 film and using an electrolyte consist of 0.05 M I_2/0.5 M LiI/0.5 M 4-*tert*-butylpyridine in 3-methoxypropionitrile solution. The photovoltaic performances of the solar cells, under AM 1.5 solar irradiation (85 $mWcm^{-2}$) with an effective light exposure area of 1 cm^2, were shown in Figure 5a and the corresponding solar cell parameters, such as short-circuit current density (J_{sc}), open-circuit voltage (V_{oc}), fill factor (FF), efficiency (η), and other relevant data are summarized in Table 2.

According to Figure 5a, it is clear that the efficiency of the fabricated DSSCs can be affected by the acceptor and π–spacer modification in the synthesized dye molecules. DSSCs fabricated with the synthesized dyes without cyanovinyl thiophene unit (EC, ER, and EB) show lower efficiency, whereas the introduction of cyanovinyl thiophene unit in the corresponding dyes (ETC, ETR, and ETB) could improve the power conversion efficiency more than two times higher with the enhancement of J_{sc} and V_{oc}. This is because of the extension of conjugation and increase in the electron withdrawing nature of the dye molecules, being capable for reduced band gap, broad and red-shifted absorption with high molar extinction coefficient, and more negative LUMO, which provides sufficient driving force for the photo-induced electron transfer from the excited dye molecules to the conduction band of TiO_2 [39; 40]. Moreover, insertion of cyanovinyl thiophene unit reduces the planar nature of the dye structure which suppresses the intermolecular interactions and inhibits the back electron transfer. This may be the reason for the higher V_{oc} values of the cyanovinyl thiophene unit containing dyes compared to the parent dye molecules [19; 41]. The observed photophysical, electrochemical, and DFT results were well supporting for the achieved solar cell performance.

In the acceptor modification part, acrylic acid acceptor based dyes (EC and ETC) show high efficiency among all the dyes. Strong electron withdrawing nature and well conjugation of acrylic acid in the entire dye molecule may be the reason for such a high efficiency. In the case of rhodanine-3-acidic acid moiety based dyes (ER and ETR), the presence of $-CH_2-$ group isolates the anchoring carboxylic acid group from the dye molecule, thus prevents electron injection into TiO_2 conduction band [42]. This may be reason for the low efficiency compared to the corresponding acrylic acid acceptor based dyes. Among the synthesized dyes, the benzimidazole-5-carboxylic acid acceptor based dyes (EB and ETB) show very low efficiency, which may be due to their poor electron withdrawing nature.

Furthermore, the incident photon-to-current conversion efficiency (IPCE) for the fabricated DSSCs was plotted in Figure 5b and their corresponding data were summarized in Table 2. Fabricated DSSCs based on cyanovinyl thiophene containing dyes (ETC, ETR and ETB) shows higher IPCE values compared to the dyes without cyanovinyl thiophene unit (EC, ER, and EB), matching well with the J-V measurement study. In addition, dye loading amount on the TiO_2 surface also affects the solar cell performance which was estimated by desorption study carried out by 0.1 M NaOH in DMF/water (1:1) mixture [30]. The surface concentration (Γ) of the sensitizers was measured by UV-vis spectroscopy and the resulting data are summarized in Table 2. As shown in Table 2, acrylic acid containing dyes possessed higher dye loading amount than corresponding dyes with rhodanine-3-acetic acid and benzimidazole-5-carboxylic acid, which may be the reason for the bulky and more bend structure responsible for decrease in the dye loading amount [43]. The introduction of cyanovinyl thiophene unit also enhances the dye loading amount due to the presence of cyano group which facilitates the dye adsorption on the TiO_2 surface [44]. Therefore, fabricated DSSCs with acrylic acid based dyes (EC and ETC) show higher efficiency and IPCE.

3.6. Electrochemical impedance Analysis

The effect of acceptor and π–spacer modification in the synthesized dye molecules for DSSC was further elucidated by electrochemical impedance spectroscopy (EIS). The results of EIS illustrate the kinetics of charge transfer processes at the interfaces of the fabricated DSSCs, such as the charge recombination at the TiO_2/dye/electrolyte interface, electron transport in the TiO_2 electrode, electron transfer at the counter electrode, and I_3^- transport in the electrolyte [45]. The impedance spectra (Nyquist plots and Bode phase plots) of fabricated DSSC based on EC, ER, EB, ETC, ETR, and ETB dyes were shown in Figure 6. In the Nyquist plots, the observed semicircle corresponds to the electron transfer resistance at the TiO_2/dye/electrolyte interface. A larger radius semicircle indicates a huge charge transfer resistance and slower electron recombination between TiO_2 and electrolyte [46]. The radius of the semicircles corresponding to the ETC, ETR, and ETB dyes based DSSCs exhibited significantly larger than the EC, ER, and EB dyes based DSSCs. It implies that the insertion of cyanovinyl thiophene unit increases the charge transfer resistance and slowed down the electron recombination at the TiO_2/dye/electrolyte interfaces which may be reason for the achieved higher efficiency

In addition, the electron recombination lifetime (τ) can be calculated from Bode phase plots (figure 6(b)) by using the following equation $\tau=1/2\pi f$, where f is the frequency of the mid-frequency peak [47]. The calculated electron lifetime values are presented in Table 2.

The relatively higher electron lifetime of ETC sensitized DSSC indicates that introduction of the cyanovinyl thiophene unit in the π–spacer and carboxylic acid acceptor can effectively suppress the injected electrons recombination with the I_3^- in the electrolyte, which may enhance the photo voltage, photocurrent and the device efficiency [48].

4. Conclusions

In this article, a series of donor-π-acceptor (D-π-A) metal-free organic dyes having diethylamine moiety as donor, phenyl with and without cyanovinyl thiophene unit as a π-spacer and acrylic acid, rhodanine-3-acetic acid, and benzimidazole-5-carboxylic acid as acceptor/anchor were synthesized as photosensitizers for the dye-sensitized solar cell application. From the experimental and theoretical results, the incorporation of cyanovinyl thiophene linker is superior in broadening of absorption band with high molar extinction coefficient and negative shift of LUMO level for an effective electron injection. Due to such reasons, cyanovinyl thiophene unit containing dye (ETC) shows maximum efficiency of 3.01%, which is more than two times higher than the corresponding dye without cyanovinyl thiophene unit (EC). These results imply that the π-spacer group modification is a possible alternative to produce excellent PCE value with longer recombination resistance and high electron lifetime.

Acknowledgments

Author SA thank DST, New Delhi (Ref. No. EMR/2014/000009) and DST-FIST, New Delhi (SR/FT/CSI-190/2008 dated 16th Mar 2008) for the sanction of research fund towards development of new facilities. Author SM thank UGC, New Delhi for the sanction of Senior Research Fellowship. In addition, support from the Ministry of Science and Technology (MOST) in Taiwan under the contract number of 104-2221-E-035-004-MY3 is also acknowledged.

Supplementary material:

Spectral data and DFT data of synthesised compounds were presented here. This material is available free of charge via the Internet.

References

[1] O'Regan B, Gratzel M. A low-cost, high-efficiency solar cell based on dye-sensitized colloidal TiO_2 films. Nature. 1991; 353, 737-40.

[2] Hagfeldt A, Boschloo G, Sun L, Kloo L, Pettersson H. Dye-Sensitized Solar Cells. Chem. Rev. 2010; 110, 6595-663.

[3] Zhang S, Yang X, Numata Y, Han L. Highly efficient dye-sensitized solar cells: progress and future challenges. Energy Environ. Sci. 2013; 6, 1443-64.

[4] Liang M, Chen J. Arylamine organic dyes for dye-sensitized solar cells. Chem. Soc. Rev. 2013; 42, 3453-88.

[5] Ooyama Y, Harima Y. Photophysical and Electrochemical Properties, and Molecular Structures of Organic Dyes for Dye-Sensitized Solar Cells. ChemPhysChem. 2012; 13, 4032-80.

[6] Yao Z, Yan C, Zhang M, Li R, Cai Y, Wang P. N-Annulated Perylene as a Coplanar π-Linker Alternative to Benzene as a Low Energy-Gap, Metal-Free Dye in Sensitized Solar Cells. Adv. Energy Mater. 2014; 4, 1-9.

[7] Amacher A, Yi C, Yang J, Bircher MP, Fu Y, Cascella M, Gratzel M, Decurtins S, Liu S-X. A quinoxaline-fused tetrathiafulvalene-based sensitizer for efficient dye-sensitized solar cells. Chem. Commun. 2014; 50, 6540-42.

[8] Zhang F, Wu D, Xu Y, Feng X. Thiophene-based conjugated oligomers for organic solar cells. J. Mater. Chem. 2011; 21, 17590-600.

[9] Ren X, Jiang S, Cha M, Zhou G, Wang Z-S. Thiophene-Bridged Double D-π-A Dye for Efficient Dye-Sensitized Solar Cell. Chem. Mater. 2012; 24, 3493-99.

[10] Joly D, Pellejà L, Narbey S, Oswald F, Chiron J, Clifford JN, Palomares E, Demadrille R. A Robust Organic Dye for Dye Sensitized Solar Cells Based on Iodine/Iodide Electrolytes Combining High Efficiency and Outstanding Stability. Sci. Rep. 2014; 4, 4033.

[11] Ting H-C, Tsai C-H, Chen J-H, Lin L-Y, Chou S-H, Wong K-T, Huang T-W, Wu C-C. A Novel Amine-Free Dianchoring Organic Dye for Efficient Dye-Sensitized Solar Cells. Org. Lett. 2012; 14, 6338-41.

[12] Subbaiah M, Sekar R, Palani E, Sambandam A. One-pot synthesis of metal free organic dyes containing different acceptor moieties for fabrication of dye-sensitized solar cells. Tetrahedron Lett. 2013; 54, 3132-36.

[13] Manoharan S, Anandan S. Cyanovinyl substituted benzimidazole based (D–π–A) organic dyes for fabrication of dye sensitized solar cells. Dyes Pigm. 2014; 105, 223-31.

[14] Sirimanne PM, Tributsch H. Parameters determining efficiency and degradation of TiO_2|dye|CuI solar cells. J Solid State Chem. 2004; 177, 1789-95.

[15] Kuang D, Ito S, Wenger B, Klein C, Moser J-E, Humphry-Baker R, Zakeeruddin SM, Grätzel M. High Molar Extinction Coefficient Heteroleptic Ruthenium Complexes for Thin Film Dye-Sensitized Solar Cells. J. Am. Chem. Soc. 2006; 128, 4146-54.

[16] Watanabe M, Hagiwara H, Iribe A, Ogata Y, Shiomi K, Staykov A, Ida S, Tanaka K, Ishihara T. Spacer effects in metal-free organic dyes for visible-light-driven dye-sensitized photocatalytic hydrogen production. J.Mater. Chem. A. 2014; 2, 12952-61.

[17] Wang Z-S, Cui Y, Dan-oh Y, Kasada C, Shinpo A, Hara K. Molecular Design of Coumarin Dyes for Stable and Efficient Organic Dye-Sensitized Solar Cells. J. Phys. Chem. C. 2008; 112, 17011-17.

[18] Ying W, Guo F, Li J, Zhang Q, Wu W, Tian H, Hua J. Series of New D-A-π-A Organic Broadly Absorbing Sensitizers Containing Isoindigo Unit for Highly Efficient Dye-Sensitized Solar Cells. ACS Appl. Mater. Interfaces. 2012; 4, 4215-24.

[19] Hua Y, He J, Zhang C, Qin C, Han L, Zhao J, Chen T, Wong W-Y, Wong W-K, Zhu X. Effects of various π-conjugated spacers in thiadiazole[3,4-c]pyridine-cored panchromatic organic dyes for dye-sensitized solar cells. J. Mater. Chem. A. 2015; 3, 3103-12.

[20] Qian X, Chang W-Y, Zhu Y-Z, Wang S-S, Pan B, Lu L, Zheng J-Y. Tri(N-carbazolyl)triphenylamine-based starburst organic dyes: effects of different acceptors on the optical, electrochemical and photovoltaic properties. RSC Adv. 2015; 5, 47422-28.

[21] Urnikaite S, Malinauskas T, Bruder I, Send R, Gaidelis V, Sens R, Getautis V. Organic Dyes with Hydrazone Moieties: A Study of Correlation between Structure

and Performance in the Solid-State Dye-Sensitized Solar Cells. J. Phys. Chem. C. 2014; 118, 7832-43.

[22] Urbani M, Barea EM, Trevisan R, Aljarilla A, de la Cruz P, Bisquert J, Langa F. A star-shaped sensitizer based on thienylenevinylene for dye-sensitized solar cells. Tetrahedron Lett. 2013; 54, 431-35.

[23] Alibabaei L, Kim JH, Wang M, Pootrakulchote N, Teuscher J, Di Censo D, Humphry-Baker R, Moser JE, Yu YJ, Kay KY, Zakeeruddin SM, Gratzel M. Molecular design of metal-free D-π-A substituted sensitizers for dye-sensitized solar cells. Energy Environ. Sci. 2010; 3, 1757-64.

[24] Chou H-H, Chen Y-C, Huang H-J, Lee T-H, Lin JT, Tsai C, Chen K. High-performance dye-sensitized solar cells based on 5,6-bis-hexyloxy-benzo[2,1,3]thiadiazole. J. Mater. Chem. 2012; 22, 10929-38.

[25] Cheema H, Islam A, Han L, El-Shafei A. Influence of Number of Benzodioxan-Stilbazole-based Ancillary Ligands on Dye Packing, Photovoltage and Photocurrent in Dye-Sensitized Solar Cells. ACS Appl. Mater. Interfaces. 2014; 6, 11617-24.

[26] Wu G, Kong F, Li J, Fang X, Li Y, Dai S, Chen Q, Zhang X. Triphenylamine-based organic dyes with julolidine as the secondary electron donor for dye-sensitized solar cells. J. Power Sources. 2013; 243, 131-37.

[27] Li S-R, Lee C-P, Kuo H-T, Ho K-C, Sun S-S. High-Performance Dipolar Organic Dyes with an Electron-Deficient Diphenylquinoxaline Moiety in the π-Conjugation Framework for Dye-Sensitized Solar Cells. Chem. Eur. J. 2012; 18, 12085-95.

[28] Zhou Y, Ding L, Shi K, Dai Y-Z, Ai N, Wang J, Pei J. A Non-Fullerene Small Molecule as Efficient Electron Acceptor in Organic Bulk Heterojunction Solar Cells. Adv. Mater. 2012; 24, 957-61.

[29] Teng C, Yang X, Yang C, Tian H, Li S, Wang X, Hagfeldt A, Sun L. Influence of Triple Bonds as π-Spacer Units in Metal-Free Organic Dyes for Dye-Sensitized Solar Cells. J. Phys. Chem. C. 2010; 114, 11305-13.

[30] Gratzel M. Photoelectrochemical cells. Nature. 2001; 414, 338-44.

[31] Zhang G, Bai Y, Li R, Shi D, Wenger S, Zakeeruddin SM, Gratzel M, Wang P. Employ a bisthienothiophene linker to construct an organic chromophore for efficient and stable dye-sensitized solar cells. Energy Environ. Sci. 2009; 2, 92-95.

[32] Miehlich B, Savin A, Stoll H, Preuss H. Results obtained with the correlation energy density functionals of becke and Lee, Yang and Parr. Chem. Phys. Lett. 1989; 157, 200-06.

[33] Lee C, Yang W, Parr RG. Development of the Colle-Salvetti correlation-energy formula into a functional of the electron density. Phys. Rev. B. 1988; 37, 785-89.

[34] Becke AD. Density-functional thermochemistry. III. The role of exact exchange. J. Chem. Phys. 1993; 98, 5648-52.

[35] Ning Z, Fu Y, Tian H. Improvement of dye-sensitized solar cells: what we know and what we need to know. Energy Environ. Sci. 2010; 3, 1170-81.

[36] Kim M-J, Yu Y-J, Kim J-H, Jung Y-S, Kay K-Y, Ko S-B, Lee C-R, Jang I-H, Kwon Y-U, Park N-G. Tuning of spacer groups in organic dyes for efficient inhibition of charge recombination in dye-sensitized solar cells. Dyes Pigm. 2012; 95, 134-41.

[37] Choi H, Shin M, Song K, Kang M-S, Kang Y, Ko J. The impact of an indeno[1,2-b]thiophene spacer on dye-sensitized solar cell performances of cyclic thiourea functionalized organic sensitizers. J.Mater. Chem. A. 2014; 2, 12931-39.

[38] Marinado T, Hagberg DP, Hedlund M, Edvinsson T, Johansson EMJ, Boschloo G, Rensmo H, Brinck T, Sun L, Hagfeldt A. Rhodanine dyes for dye-sensitized solar cells : spectroscopy, energy levels and photovoltaic performance. Phys. Chem. Chem. Phys. 2009; 11, 133-41.

[39] Li J, Yang X, Cheng M, Wang M, Sun L. Phenoxazine-based panchromatic organic sensitizers for dye-sensitized solar cells. Dyes Pigm. 2015; 116, 58-64.

[40] Hung W-I, Liao Y-Y, Hsu C-Y, Chou H-H, Lee T-H, Kao W-S, Lin JT. High-Performance Dye-Sensitized Solar Cells Based on Phenothiazine Dyes Containing Double Anchors and Thiophene Spacers. Chem. Asian J. 2014; 9, 357-66.

[41] Feng Q, Zhang Q, Lu X, Wang H, Zhou G, Wang Z-S. Facile and Selective Synthesis of Oligothiophene-Based Sensitizer Isomers: An Approach toward Efficient Dye-Sensitized Solar Cells. ACS Appl. Mater. Interfaces. 2013; 5, 8982-90.

[42] Echeverry CA, Herranz MA, Ortiz A, Insuasty B, Martin N. Rhodanine-3-acetic acid and π-extended tetrathiafulvalene (exTTF) based systems for dye-sensitized solar cells. New J. Chem. 2014; 38, 5801-07.

[43] Kumar D, Justin Thomas KR, Lee C-P, Ho K-C. Organic Dyes Containing Fluorene Decorated with Imidazole Units for Dye-Sensitized Solar Cells. J. Org. Chem. 2014; 79, 3159-72.

[44] Katono M, Bessho T, Wielopolski M, Marszalek M, Moser J-E, Humphry-Baker R, Zakeeruddin SM, Grätzel M. Influence of the Anchoring Modes on the Electronic and Photovoltaic Properties of D−π–A Dyes. J. Phys. Chem. C. 2012; 116, 16876-84.

[45] Qian X, Gao H-H, Zhu Y-Z, Lu L, Zheng J-Y. Biindole-based double D-π-A branched organic dyes for efficient dye-sensitized solar cells. RSC Adv. 2015; 5, 4368-75.

[46] Wu K-L, Li C-H, Chi Y, Clifford JN, Cabau L, Palomares E, Cheng Y-M, Pan H-A, Chou P-T. Dye Molecular Structure Device Open-Circuit Voltage Correlation in Ru(II) Sensitizers with Heteroleptic Tridentate Chelates for Dye-Sensitized Solar Cells. J. Am. Chem. Soc. 2012; 134, 7488-96.

[47] Qian X, Gao H-H, Zhu Y-Z, Lu L, Zheng J-Y. 6H-Indolo[2,3-b]quinoxaline-based organic dyes containing different electron-rich conjugated linkers for highly efficient dye-sensitized solar cells. J. Power Sources. 2015; 280, 573-80.

[48] Kim SH, Choi J, Sakong C, Namgoong JW, Lee W, Kim DH, Kim B, Ko MJ, Kim JP. The effect of the number, position, and shape of methoxy groups in triphenylamine donors on the performance of dye-sensitized solar cells. Dyes Pigm. 2015; 113, 390-401.

Table 1. Optical, electrochemical data and HOMO, LUMO energy levels of synthesised dyes.

S.No	Dye	λ_{abs}/nm (ε/$M^{-1}cm^{-1}$)[a]	λ_{em} (nm)[a]	Stokes shift (nm)	E_{HOMO} (eV)[b]	E_{0-0} (eV)[c]	E_{LUMO} (eV)[d]	E_{ox}/V (Vs.Fc)
1	EC	367 (35550)	445	78	-4.98	3.05	-1.93	0.71
2	ER	458 (35750)	550	92	-5.09	2.48	-2.61	0.82
3	EB	352 (29014)	421	69	-5.23	3.28	-1.97	0.96
4	ETC	470 (45424)	570	100	-4.90	2.37	-2.53	0.63
5	ETR	531 (47163)	662	131	-5.02	2.02	-3.00	0.75
6	ETB	460 (41962)	540	80	-5.08	2.45	-2.63	0.81

[a]Absorption and emission spectra were measured in DMF. [b]The oxidation potential of the dyes was measured under the following conditions: glassy carbon working electrode, 0.1 M TBAP in DMF as an electrolyte, scan rate of 100 mV/s. Potentials measured *vs* Fc/Fc^+ were converted to NHE by addition of +0.53 V. [c]The $E_{(0-0)}$ are estimated from the intercept of the absorption and emission spectra. [d]The excited state oxidation potentials were derived from the equation: $\mathbf{E_{(LUMO)} = E_{(HOMO)} + E_{(0-0)}}$.

Table 2. DSSC Performance Parameters of the synthesised dyes.

Dye	J_{sc} ($mAcm^{-2}$)	Voc (mV)	FF	Efficience (Ƞ) (%)	IPCE (%)	Electron lifetime (τ) (ms)	Surface concentration (Γ) (mol/cm^2)
EC	2.83	670	0.62	1.38	23.13 (371 nm)	9.04	1.68×10^{-7}
ER	2.27	529	0.59	0.82	20.26 (450 nm)	2.79	0.98×10^{-7}
EB	0.54	567	0.61	0.22	15.50 (355 nm)	2.30	1.12×10^{-7}
ETC	5.71	689	0.65	3.01	55.01 (450 nm)	14.01	2.35×10^{-7}
ETR	3.88	597	0.63	1.73	32.36 (495 nm)	10.80	1.35×10^{-7}
ETB	1.50	614	0.58	0.63	19.48 (440 nm)	4.42	1.57×10^{-7}

Figure 1

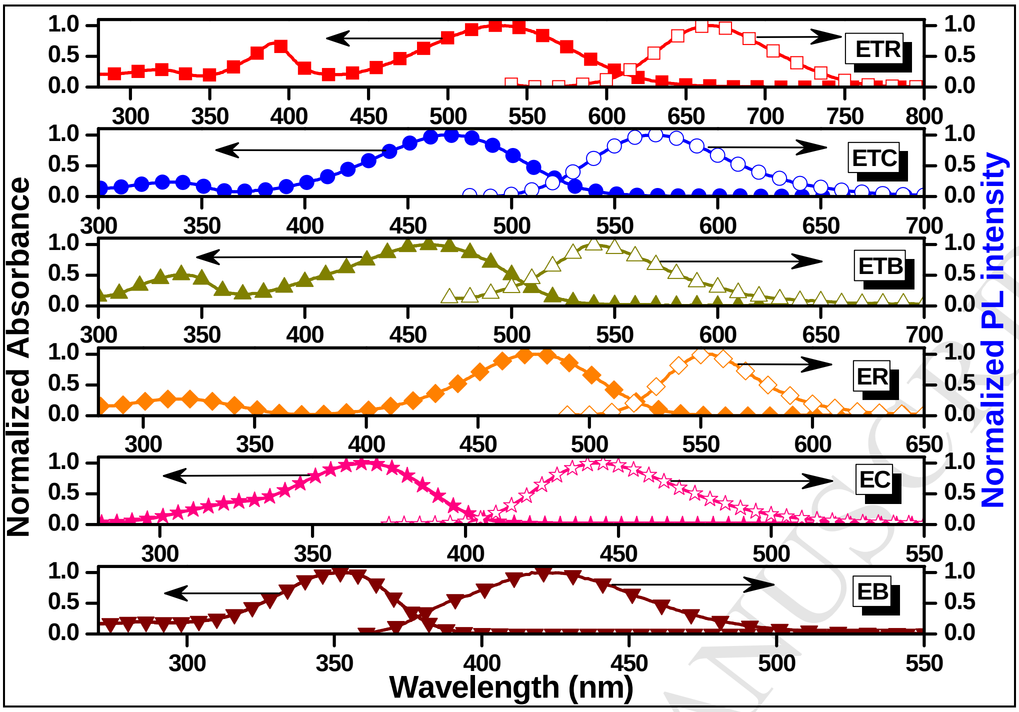
Normalized Absorbance
Normalized PL intensity
ETR
ETC
ETB
ER
EC
EB
1.0
0.5
0.0
300
350
400
450
500
550
600
650
700
750
800
Wavelength (nm)

Figure 2

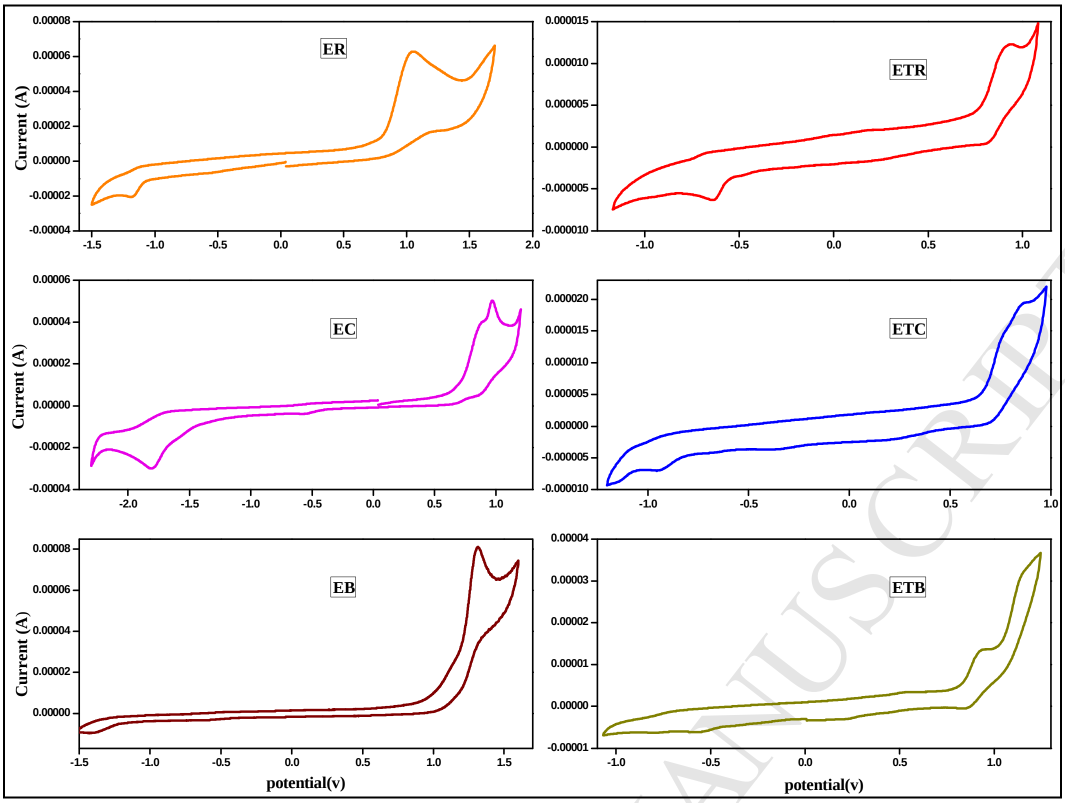
ER
ETR
EC
ETC
EB
ETB
Current (A)
Current (A)
Current (A)
potential(v)
potential(v)
0.00008
0.00006
0.00004
0.00002
0.00000
-0.00002
-0.00004
0.000015
0.000010
0.000005
0.000000
-0.000005
-0.000010
0.000020
0.00004
0.00003
0.00002
0.00001
-0.00001
-2.0
-1.5
-1.0
-0.5
0.0
0.5
1.0
1.5
2.0

Figure 3

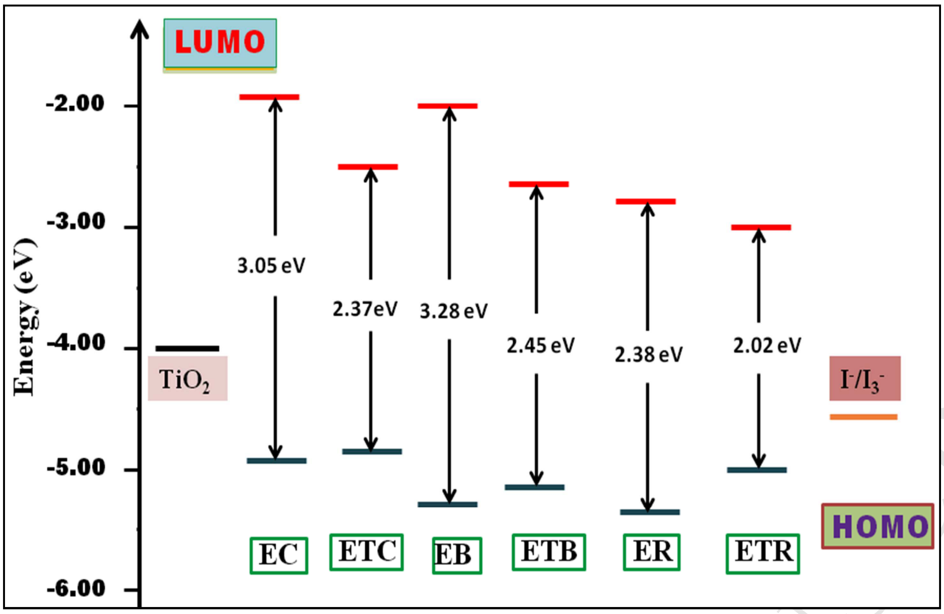
LUMO
-2.00
-3.00
-4.00
-5.00
-6.00
Energy (eV)
TiO$_2$
3.05 eV
2.37eV
3.28 eV
2.45 eV
2.38 eV
2.02 eV
I$^-$/I$_3^-$
HOMO
EC
ETC
EB
ETB
ER
ETR

Figure 4

Dye	Optimized structure	HOMO	LUMO
EC	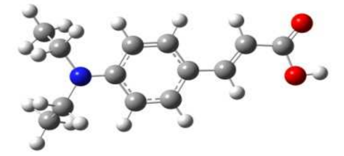	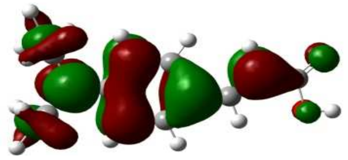	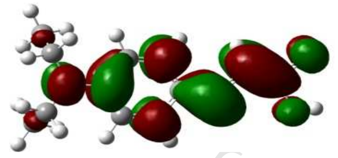
ER	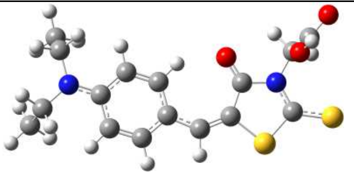	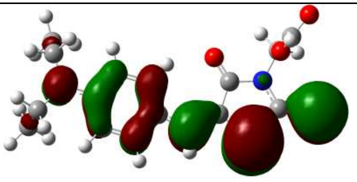	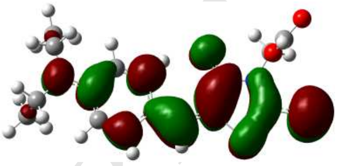
EB	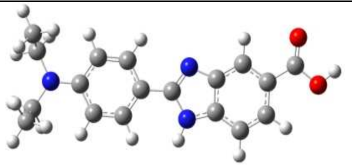	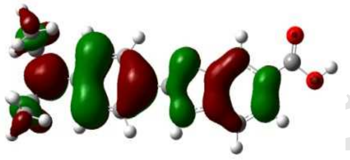	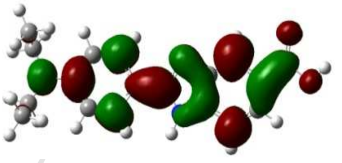
ETC	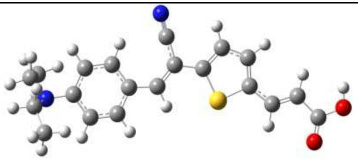	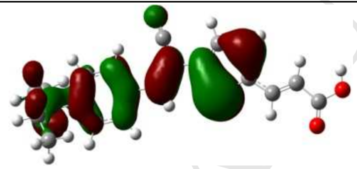	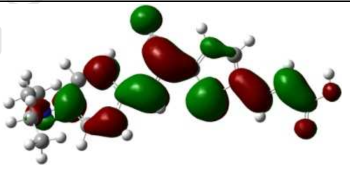
ETR	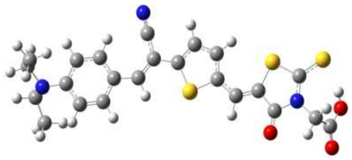	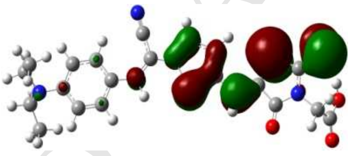	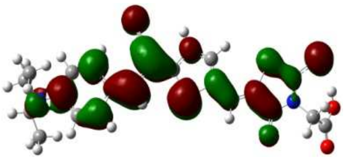
ETB	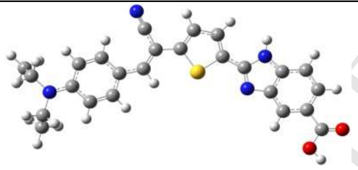	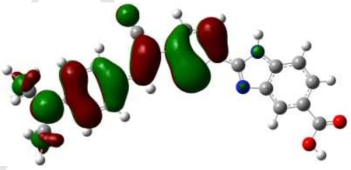	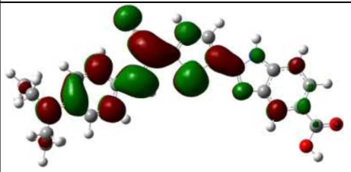

Figure 5

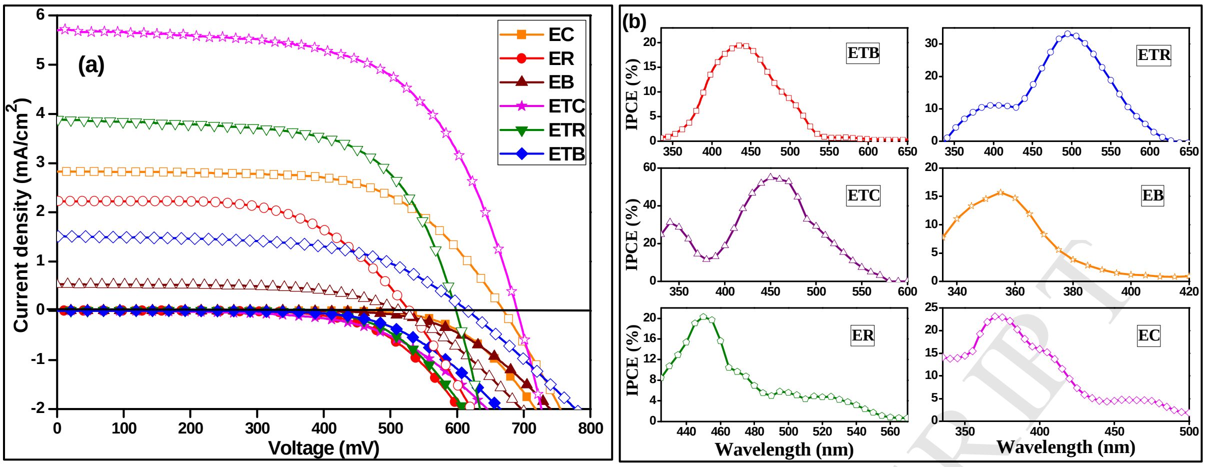
(a)
Current density (mA/cm^2)
Voltage (mV)
6
5
4
3
2
1
0
-1
-2
0
100
200
300
400
500
600
700
800
EC
ER
EB
ETC
ETR
ETB
(b)
ETB
ETR
ETC
EB
ER
EC
IPCE (%)
Wavelength (nm)

Figure 6

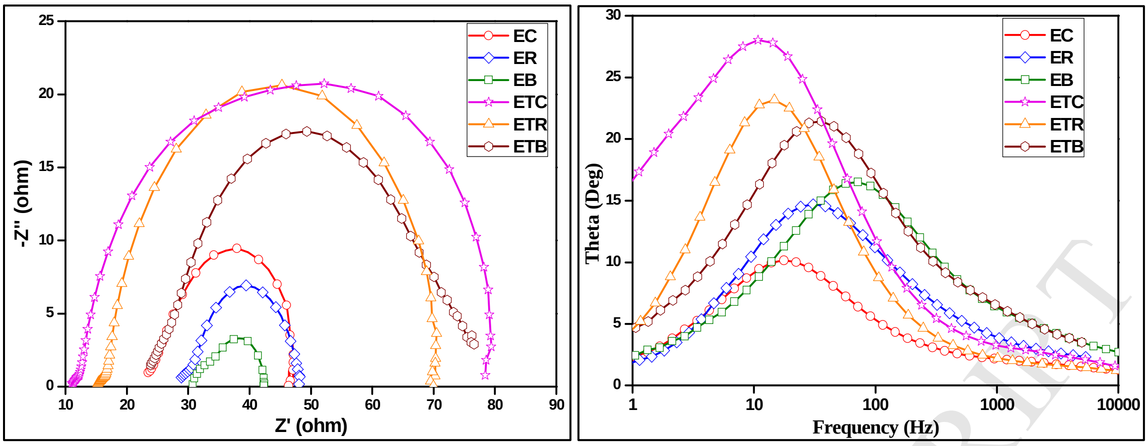
-Z'' (ohm)
Z' (ohm)
0
5
10
15
20
25
10
20
30
40
50
60
70
80
90
EC
ER
EB
ETC
ETR
ETB
Theta (Deg)
Frequency (Hz)
0
5
10
15
20
25
30
1
10
100
1000
10000
EC
ER
EB
ETC
ETR
ETB

Scheme 1

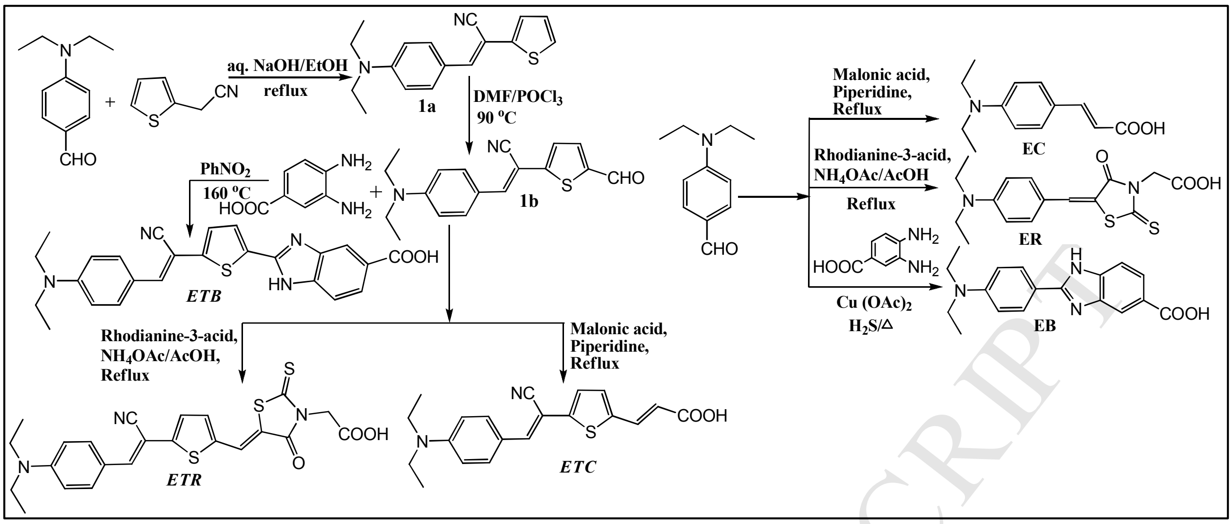
aq. NaOH/EtOH
reflux
1a
DMF/POCl3
90 °C
1b
PhNO2
160 °C
ETB
Rhodianine-3-acid,
NH4OAc/AcOH,
Reflux
ETR
Malonic acid,
Piperidine,
Reflux
ETC
Malonic acid,
Piperidine,
Reflux
EC
Rhodianine-3-acid,
NH4OAc/AcOH
Reflux
ER
Cu (OAc)2
H2S/Δ
EB

Captions for Figures and Schemes

Figure 1. Normalized UV-visible absorption and emission spectra of EC, ER, EB, ETC, ETR and ETB dyes recorded in DMF medium ($5x10^{-5}M$)

Figure 2. Cyclic voltammograms of dyes measured in DMF solutions with TBAP (0.1 M) as the electrolyte (working electrode: GC; reference electrode: Ag wire; counter electrode: Pt wire; scan rate: 100 mVs^{-1})

Figure 3. Energy level diagram of synthesized dyes based on absorption, emission and electrochemical data

Figure 4. Optimized ground-state geometries and the frontier molecular orbitals of the HOMO and LUMO levels calculated with B3LYP/6-31G (d) of synthesized dyes

Figure 5. Photocurrent–voltage (a) and IPCE (b) spectra of DSSC based on EC, ER, EB, ETC, ETR and ETB dyes

Figure 6. Electrochemical impedance spectra of DSSCs measured at $85mWcm^{-2}$. (a) Nyquist plots. (b) Bode phase plots

Scheme 1. Molecular structures and synthetic procedure of the EC, ER, EB, ETC, ETR, and ETB Dyes

Highlights

- Synthesis of metal-free organic dyes using cyanovinyl thiophene unit and acceptors
- Dyes were synthesized from low cost starting materials
- Cyanovinyl thiophene unit and acrylic acid containing DSSC shows higher efficiency